Pure Appl. Chem., Vol. 84, No. 11, pp. 2183–2202, 2012.
http://dx.doi.org/10.1351/PAC-CON-11-10-36

A unique, two-component sensing system for fluorescence detection of glucose and other carbohydrates*

David B. Cordes[1,‡] and Bakthan Singaram[2]

[1]*Department of Chemistry, Pacific University, Forest Grove, OR 97116, USA;*
[2]*Department of Chemistry and Biochemistry, University of California, Santa Cruz, CA 95102, USA*

Abstract: In our glucose-sensing system, a boronic acid-modified viologen molecule quenches the fluorescence of a separate dye molecule. When glucose or other monosaccharides are added and bind to the boronic acid, the quenching ability of the viologen is diminished and fluorescence increases. Thus, changes in the fluorescence of the dye can be correlated with changing glucose concentration. Quenching and sugar-sensing results are explained by an electrostatic interaction between dye and quencher. This modular system can be configured in a nearly unlimited number of ways through substitution and multiplexing of the two fundamental quencher and dye components. Significantly, fluorescent quantum dots (QDs) can also be used as the reporter component. The system can also be immobilized in a hydrogel polymer to provide real-time, reversible sugar sensing.

Keywords: biomedical applications; boron; carbohydrates; chemical sensors; fluorescence; sensors.

INTRODUCTION

Fluorescent boronic acid-based glucose sensors

Since the first simple thermometers and barometers were prepared by Galileo and his contemporaries, sensing technology has greatly expanded the ability of humankind to explore the physical world and helped to reveal the mystery of Nature. Many of the most interesting new examples of such sensing technology have emerged from efforts to monitor the concentrations of physiologically important species using electrochemical and optical methods. Particular effort has been made toward the determination of glucose concentrations under physiological conditions [1,2]. A very large number of these glucose sensors have relied on a combination of a boronic acid-based glucose receptor coupled with a fluorescence reporting system. Boronic acids are used as receptors because they are able to reversibly form covalent complexes with diols and polyols such as glucose and fructose [3–7]. Equilibria between arylboronic acids and generic diols are shown in Scheme 1.

Significantly, the pK_a of the boron typically decreases by 1 or 2 units when boronic acids are converted to boronic esters. For example, in the case of simple phenylboronic acid, the pK_a drops from ~8.8 to 6.5 upon binding of glucose, but on binding of fructose the pK_a drops even further, all the way to 4.5 [8]. Thus, the particular distribution of species depicted in Scheme 1 can be controlled by adjustments

Pure Appl. Chem.* **84, 2183–2498 (2012). A collection of invited papers based on presentations at the 14th International Meeting on Boron Chemistry (IMEBORON-XIV), Niagara Falls, Canada, 11–15 September 2011.
‡Corresponding author

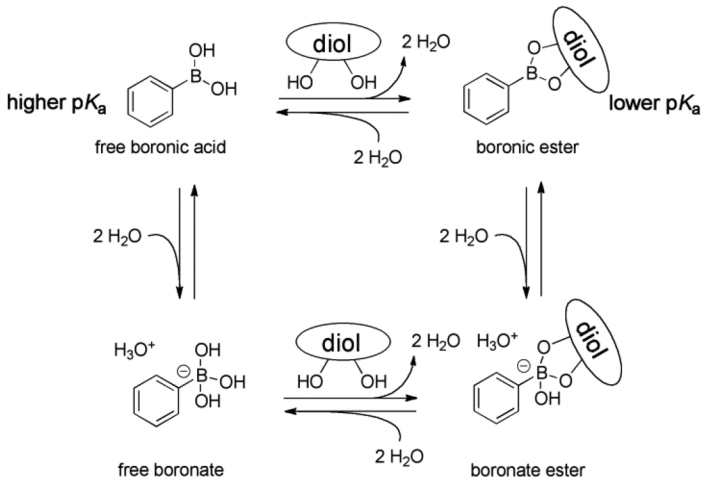

Scheme 1 Boronic acid equilibria for generic diols.

in pH and diol concentration. If the pK_a of a boronic acid is well above the ambient pH it will exist exclusively in its trigonal neutral state. Binding of a diol to the neutral, trigonal boronic acid at this ambient pH can result in a boronate ester, which, with its lower pK_a, will convert rapidly to the "-ate" form in which the boron is tetrahedral and anionic [9,10]. In nearly all boronic acid sensor systems for glucose, it is this binding event and associated electronic and steric changes around the boronic acid receptor that cause a change in the fluorescence emission that can then be correlated with glucose concentrations. Accordingly, these systems can be considered in terms of two key elements: a boronic acid receptor and a fluorescent reporter.

The majority of boronic acid-based sensor systems combine the boronic acid receptor and fluorescent reporter elements in a single molecule. These so-called one-component sensors include a number of highly sensitive and diverse systems developed over the past two decades [11–19]. However, several multicomponent systems have been developed including our own two-component sensing system [20,21]. Compared with the more common single-molecule approach to fluorescence-based saccharide sensors, the two-component approach favored by our group relies on using saccharide binding to a boronic acid receptor in order to modulate a fluorescence-dependent interaction between the fluorophore and a second molecule. This two-component approach removes the synthetic difficulties associated with combining the fluorophore and receptor in a single sensor molecule and allows for considerable versatility in choosing each component.

In the two-component saccharide sensing system developed by the Singaram group, boronic acid-functionalized viologen quenchers are used as the saccharide receptor unit. In this system, the cationic viologen is first used to quench the fluorescence of an anionic fluorescent dye through formation of a nonfluorescent ground-state complex. Binding of a diol, such as glucose, to the boronic acid of the viologen causes dissociation of the complex and diminishes the efficiency with which the fluorescence emission is quenched. Thus, the intensity of fluorescence emission can be correlated with the concentration of glucose or whatever diol or monosaccharide is being tested [22]. The typical fluorescence responses of our system are illustrated in Fig. 1.

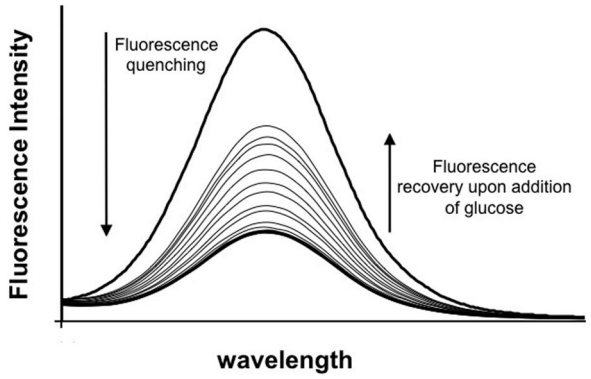

Fig. 1 Characteristic fluorescence responses of our glucose-sensing system.

In our early studies, we relied largely on the anionic dye pyranine, 8-hydroxy-1,3,6-pyrenetrisulfonic acid trisodium salt (HPTS), as the fluorophore and a boronic acid-substituted viologen as the receptor. HPTS is a photostable, anionic, and highly water-soluble green-fluorescing dye with a quantum yield of nearly one. Viologens, the cationic salts of 4,4'-bipyridinium, are well-known electron acceptors that have been found to quench the fluorescence of numerous dyes [23–25] and macromolecular systems [26–29]. The quenching of HPTS fluorescence by viologen quenchers was first reported by Baptista who studied complexation of the dye with methylviologen (MV^{2+}) [23]. In our earliest studies, we found that anionic HPTS and its derivatives were generally sensitive to quenching by boronic acid-substituted viologens and by related phenanthrolinium compounds. It was also determined that by changing the concentration of glucose and other monosaccharides, the fluorescence intensity of a quenched solution of dye could be modulated to provide a sensing signal [22,30]. A general mechanism that accounts for both fluorescence quenching and saccharide sensing is depicted in Scheme 2.

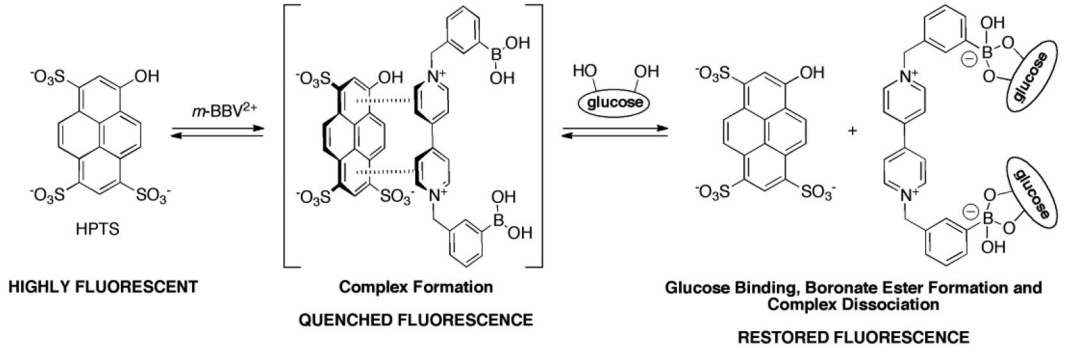

Scheme 2 Proposed glucose-sensing mechanism showing initial complexation of HPTS and *m*-BBV^{2+} to produce a nonfluorescent ground-state complex, followed by glucose binding and dissociation of the complex to produce a fluorescent signal.

In the example given in Scheme 2, the viologen quencher/receptor molecule is a boronic acid-substituted viologen, 4,4'-*N,N'*-bis(benzyl-3-boronic acid)-bipyridinium dibromide, commonly called: *m*-BBV^{2+}. This viologen is doubly charged at physiological pH of 7.4. In this cationic state, the boron substituents are trigonal and neutral, and the viologen forms a nonfluorescent ground-state complex with anionic fluorescent dye HPTS. Upon sugar binding, the pK_a of boron in its ester configuration is lowered, causing the boron to convert to its tetrahedral, anionic form in which it bears a charge of –1.

This change, which has been confirmed with ^{11}B NMR, causes the viologen quencher to become electronically neutral and results in dissociation of the complex. Thus, fluorescence is restored as the complex dissociates and the quenching interaction is diminished. To summarize, in this glucose-sensing system, signal transduction derives from two separate, but interdependent, reversible complexation reactions. The first is complexation of a fluorescent dye with a viologen, which quenches the fluorescence. The second is the binding of the sugar to the boronic acid receptor of the viologen, which causes the initial dye:quencher complex to dissociate and fluorescence emission to recover.

VARIATIONS IN THE VIOLOGEN-BASED QUENCHER/RECEPTOR

In our initial studies, we prepared a series of boronic acid-modified viologen quenchers to examine the effects of boronic acid positioning, quencher charge, and quencher-to-dye (Q:D) ratio on fluorescence quenching and glucose sensing. We first prepared simple, symmetrical dicationic viologen quenchers with two boronic acid receptor groups arranged in the ortho, meta, and para positions (*o*-BBV^{2+}, *m*-BBV^{2+}, and *p*-BBV^{2+}) (Fig. 2). We were interested in how these three arrangements would affect fluorescence quenching and glucose sensing and hypothesized that the signal magnitude and saccharide selectivity might be affected.

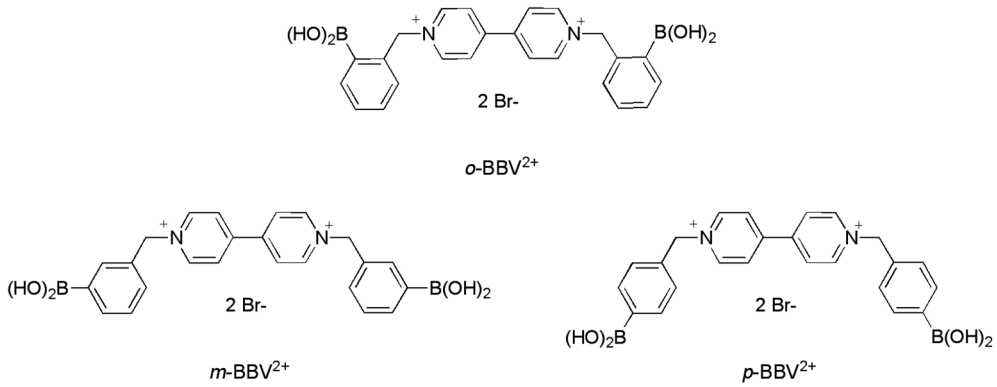

Fig. 2 Symmetrically substituted boronic acid-modified viologen quenchers.

Effects of boronic acid positioning

When we evaluated this series of variously substituted boronic acid-modified viologen quenchers, we observed only minor differences in their ability to quench the fluorescence of HPTS, with the *para*-substituted *p*-BBV^{2+} providing the most significant quenching. Figure 3 shows results of the fluorescence-quenching experiments using a Stern–Volmer plot, in which the steepness of the slope correlates positively with the degree of quenching.

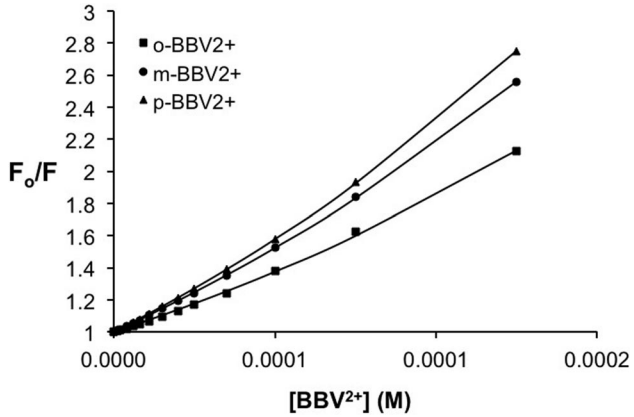

Fig. 3 Stern–Volmer plot showing quenching effects using variously substituted boronic acid-modified viologens to quench the fluorescence of HPTS (4×10^{-6} M) at pH 7.4. λ_{ex} = 460 nm, λ_{em} = 510 nm; F_o = original fluorescence; F = fluorescence after addition of quencher.

Glucose binding studies of *o*-BBV^{2+}, *m*-BBV^{2+}, and *p*-BBV^{2+}

After evaluation of this series of viologens for their fluorescence quenching, we carried out a set of optimization experiments to determine the effects of Q:D ratio on glucose sensing. Initial work established that good sugar-sensing results could be obtained after first substantially quenching the HPTS with a 30:1 Q:D ratio. When the three viologens were tested for their response to glucose at this 30:1 ratio, we found a fair degree of variation in the results, with *o*-BBV^{2+} giving the greatest signal. Significantly, this was the compound that had provided the weakest quenching among the three. We suspect that this may be a consequence of a unique charge–neutralization interaction that can occur in *o*-BBV^{2+} between the boron and the positively charged nitrogen of the viologen [31]. The *meta*- and *para*-substituted viologens gave a smaller, but still significant response in the physiological range. The superimposed relative fluorescence increase of all three quenchers is shown in Fig. 4.

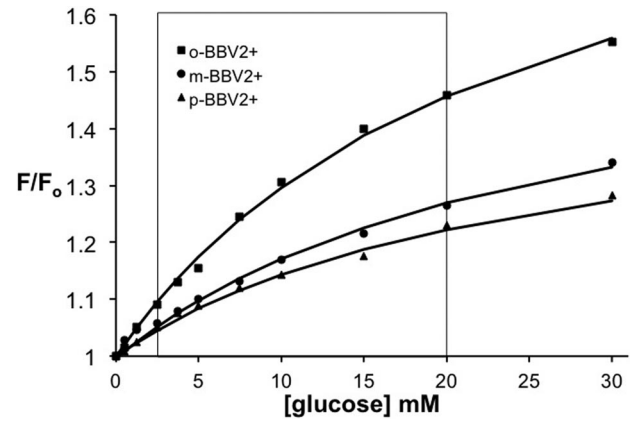

Fig. 4 Glucose response of *o*-, *m*-, and *p*-BBV^{2+} in combination with HPTS (4×10^{-6} M) at the same Q:D ratio of 30:1 in pH 7.4 aqueous solution. Human physiological glucose range is boxed. λ_{ex} = 460 nm, λ_{em} = 510 nm.

Monosaccharide binding studies were carried out using fructose and galactose as well, but they all demonstrated essentially the same fructose >> galactose > glucose selectivity as that observed for simple phenylboronic acid. These early results suggested that achieving glucose selectivity in our system might be overly difficult given the limitations of the 4,4'-bipyridinium structure at the core of our receptor. Additional experimentation with mixed boronic acid substitution patterns based on the 4,4'-bipyridinium failed to provide any significant deviations from the aforementioned selectivity. Eventually, however, systematic exploration of new receptor structures led to the development of a special viologen based on 3,3'-bipyridine that showed both good signal response and a remarkable and rarely observed selectivity for glucose over fructose and a number of other carbohydrates (Fig. 5) [32].

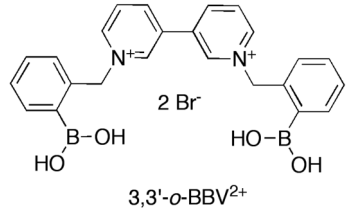

Fig. 5 Structure of the glucose-selective sensor component 3,3'-*o*-BBV^{2+}.

After some time, a modest library of over 20 structurally unique, boronic acid-modified viologens was prepared. These included variously substituted viologens based on the 3,3', 3,4', and 4,4' bipyridinium cores and a series of interesting bis-viologens in which two bipyridinium units were combined in a single compound [31–33]. In terms of both signal magnitude and selectivity, many of these had similar responses when evaluated with selected sets of carbohydrates. Several of these, however, including mainly viologens with *ortho*-substituted boronic acids, showed particularly unique patterns in their signal responses. Further study showed that by using linear discriminant analysis, a set of as few as three viologen quencher molecules could be used in an array-type configuration to discriminate accurately among 12 saccharides [34]. A similar array of 3 viologens proved itself able to differentiate between various phospho sugars, nucleotides, and saccharides [35]. Additional work also revealed that certain viologens functioned ideally in applications for enzyme assays in which the system was able to provide information about the enzymes sucrose phosphorylase and phosphoglucomutase based on detection of their saccharide byproducts [36]. While the positioning of boronic acids clearly has a major effect on the sugar-sensing and quenching ability, we were also curious about the effects of viologen charge on the sensing properties of the system.

Effects of quencher charge

As the proposed mechanism suggests, the quenching process appears heavily dependent on the degree of electrostatic attraction between the cationic viologen quencher and anionic fluorescent dye. All of our earlier studies had demonstrated the importance of charge interactions in our sensing system and suggested that the number of charges on the viologen quencher/receptor play a major role in determining quenching and sugar-sensing behavior. So, a series of experiments was conducted to carefully examine the effects of viologen charge on the sensing system [37]. Initial work was done to prepare a set of variously charged, but structurally similar boronic acid-modified viologen quenchers (Fig. 6).

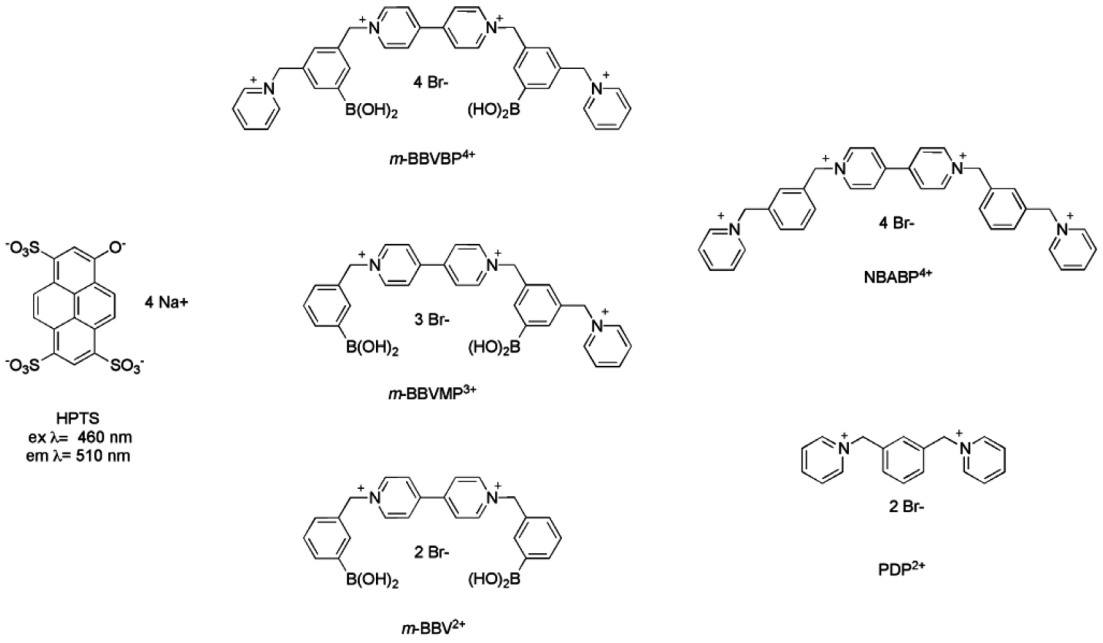

Fig. 6 Structures of HPTS and some of the viologen quenchers used in the study.

In the first of these studies, the boronic acid-substituted viologens were used to quench the fluorescence of HPTS. Results are shown in Fig. 7.

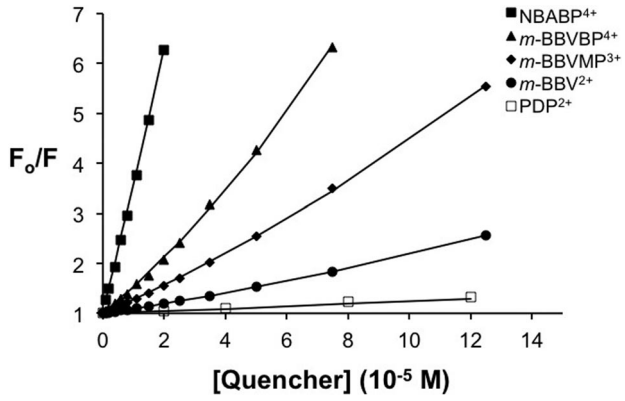

Fig. 7 Stern–Volmer plot of fluorescence quenching of HPTS (4×10^{-6} M) by quenchers at pH 7.4 with charges indicated. Studies conducted at 20 °C, λ_{ex} = 460 nm, λ_{em} = 510 nm; F_o = original fluorescence; F = fluorescence after addition of quencher.

It appears that more positively charged viologens have either greater electron affinity or a stronger electrostatic attraction through which they can bind HPTS in a nonfluorescent quencher:dye complex, or both. The viologens studied demonstrated extremely efficient quenching. Observed quenching was determined by graphical methods to be due to a predominantly static quenching mechanism in which the viologen quencher deactivates dye fluorescence through formation of a nonfluorescent complex. Such static quenching is contrasted with dynamic quenching, in which the fluorophore is deactivated

through fleeting, collisional interactions with quencher molecules. That our system operates via static and not dynamic quenching was confirmed with temperature experiments and through absorbance studies, the latter of which provided binding constants in good agreement with those obtained from the fluorescence quenching studies.

Sugar sensing and the effects of Q:D ratios

A considerable benefit of the two-component system is the ability to vary the Q:D ratio in order to optimize both the magnitude of the sensor response and its sensitivity in the concentration range of interest. When the ratio between quencher and dye is steadily increased for each in a series of glucose titrations, a pattern emerges in which the point at which the system saturates steadily shifts to higher glucose concentrations. This makes the binding isotherm more linear in the low concentration range and is illustrated in Fig. 8.

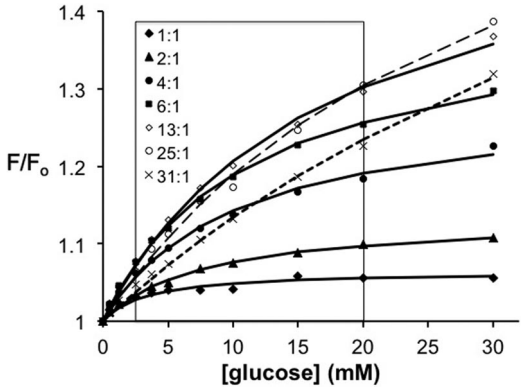

Fig. 8 Binding isotherms for different Q:D ratios from fluorescence data for addition of glucose to a sample of HPTS (4×10^{-6} M) quenched by *m*-BBVBP^{4+} at pH 7.4. Physiological glucose range is boxed.

As is evident in Fig. 8, the low Q:D ratios such as 1:1 and 2:1 give weak signals and relatively saturated responses in the physiological range of glucose concentration (2.5–20 mM). Higher Q:D ratios, however, provide an isotherm that is increasingly linear in the physiological range of interest. At 25:1 and 31:1, the signal response in the physiological range drops from a maximum reached at 13:1, but the linearity is improved across the same region. All of the quenchers studied displayed similar behavior with respect to Q:D ratios.

For glucose sensor applications, a dynamic, but linear response across the physiological glucose range is highly desirable so that a fluorescence change can be easily correlated with changes in glucose concentration. The ability to tune the signal response for a particular concentration range circumvents a common problem of many fluorescence-based systems in which there may be excellent sensitivity at low concentrations, but the signal response is too rapidly saturated before physiological glucose concentrations are even reached. For this reason, we adjusted Q:D ratios for each of the quencher-dye combinations in order to obtain a linear response across the physiological range. We found that *m*-BBVBP^{4+} gave optimal results with HPTS at a Q:D ratio of 31:1, while *m*-BBVMP^{3+} and *m*-BBV^{2+} worked best at a ratio of 125:1. The apparent glucose binding constants for *m*-BBV^{2+}, *m*-BBVMP^{3+}, *m*-BBVBP^{4+} determined from the fluorescence data at the optimized ratios were, respectively, 11 ± 3, 12 ± 2, and 27 ± 6 M^{-1}. The optimized apparent glucose binding isotherms for these viologens are shown in Fig. 9.

A number of additional studies were carried out exploring a wide variety of quenchers based on variously substituted bipyridinium [31–33] and phenanthrolinium [30] species. Together, with the work

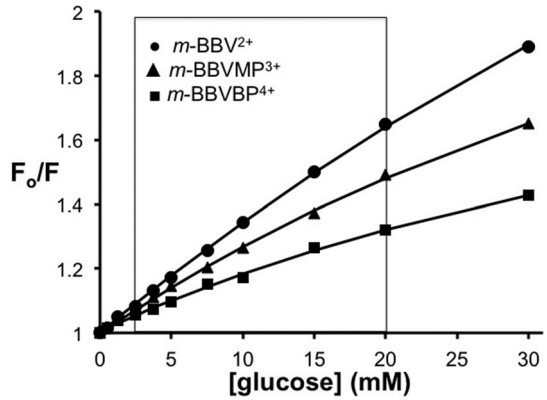

Fig. 9 Glucose response of viologens with HPTS (4×10^{-6} M) at pH 7.4; optimized Q:D ratios for *m*-BBV^{2+}, *m*-BBVMP^{3+}, and *m*-BBVBP^{4+} with HPTS were, respectively, 31:1, 125:1, and 125:1.

described above, these studies demonstrate the considerable versatility possible with respect to the receptor component in this system. The next section demonstrates how similar flexibility and versatility can be achieved with respect to the fluorophore component.

VARIATIONS IN THE FLUOROPHORE

Having explored variation in the receptor component of our system, we then turned to experiments in which the fluorescent reporter component was varied while keeping the viologen-based receptor constant. Additional experiments explored how multiple dyes could be used simultaneously with a single viologen-based receptor and how other fluorophores, such as fluorescent quantum dots (QDs), could be used in this system.

Many fluorescence-based sensing systems rely on a single molecule in which the fluorophore is synthetically combined with the receptor unit in a single molecule. Thus, there is not much leeway for the introduction of new fluorophores into these systems without considerable synthetic manipulation. Even when such modification is relatively easy, the photophysical properties of the fluorophore may undergo significant changes upon addition of the new receptor moiety. Our two-component monosaccharide-sensing system overcomes these limitations in that the receptor unit is not attached to the fluorophore, but to a separate fluorescence-quenching moiety. So, in our system, one dye can easily be substituted for another and with predictable results in terms of the photophysical behavior of the new fluorophore.

The ability to substitute various dyes for HPTS confers important advantages on our two-component system. First, such dye substitution allows for use of nearly any wavelength for *excitation* of the fluorophore. This is a considerable advantage since particular biological applications might preclude the use of damaging UV excitation wavelengths. Such freedom of substitution also allows for simultaneous use of multiple dyes. In such a case, dyes with a shared excitation wavelength can be excited by the same light source, thus allowing for dual signal and ratiometric fluorescence sensing applications.

The ability to choose fluorophores with certain *emission* wavelengths is also a highly desirable quality of the two-component sensing system. Selection of an emission wavelength might depend on interfering effects due to absorbance of other sensor components. As suggested, it may also be practical to use more than a single dye in some applications, such as for dual signal or ratiometric sensing. To explore the potential for realizing some of these benefits, we carried out studies on the use of various organic fluorophores in our two-component sensing system. In the first of these studies, we demon-

strate the versatility of the sensing system by using a broad range of anionic fluorescent dyes in combination with a boronic acid-modified viologen quencher at pH 7.4 [38].

Glucose sensing across the visible spectrum with *m*-BBVBP^{4+} and anionic fluorescent dyes

Structurally diverse ionic dyes were selected to provide a wide range of emission wavelengths. All the dyes possess at least one sulfonic or carboxylic acid group and were expected to exist in their anionic forms at pH 7.4. Some of the dyes used in this study are shown in Fig. 10.

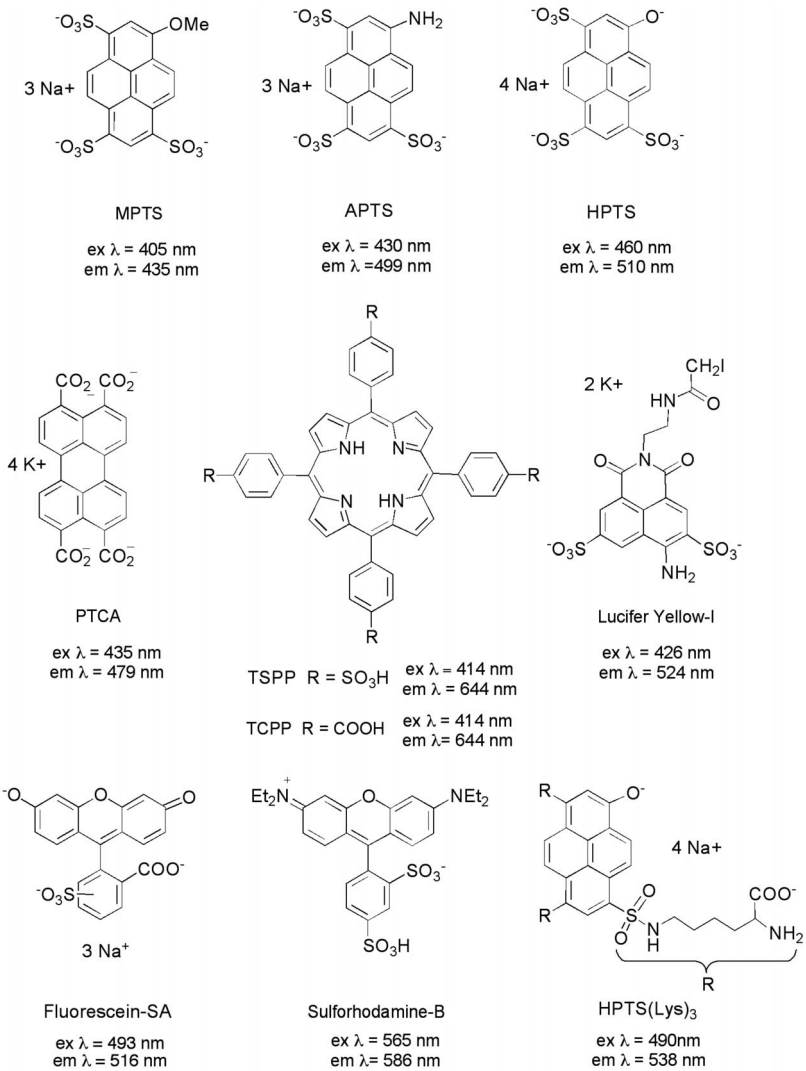

Fig. 10 Anionic dyes used in saccharide sensing. All compounds are shown as purchased or prepared. MPTS = methoxypyrenetrisulfonic acid, trisulfonate; PTCA = perylenetetracarboxylic acid, tetracarboxylate; HPTS = hydroxypyrenetrisulfonic acid, trisulfonate; APTS = aminopyrenetrisulfonic acid, trisulfonate; fluorescein-SA = fluorescein-5-(and-6-) sulfonic acid; lucifer yellow-I = lucifer yellow iodoacetamide; SR-B = sulforhodamine-B; HPTS(Lys)$_3$ = hydroxypyrenetri(lysine)sulfonamide; and TCPP = tetrakis(4-carboxyphenyl)porphine; TSPP = tetrakis(4-sulfophenyl)porphine.

The emission spectra of selected dyes used in this study are shown in Fig. 11.

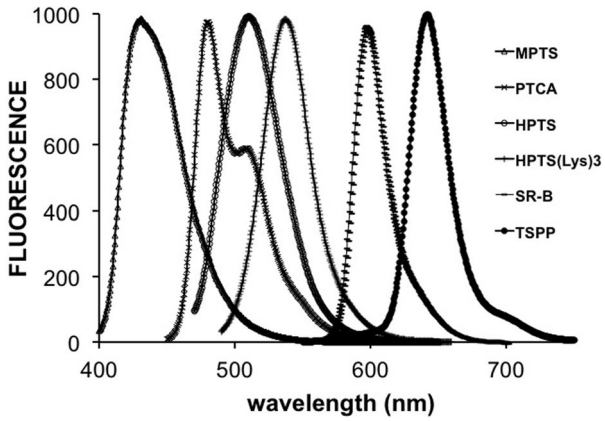

Fig. 11 Emission spectra of selected dyes in pH 7.4 buffer.

We selected the highly charged *m*-BBVBP^{4+} for this study because we knew it was an extremely good quencher. We anticipated that this would be an advantage in this study since some of the selected dyes possessed only a small degree of negative charge at physiological pH and, thus, would be expected to undergo only a minor amount of quenching through electrostatic complexation with the quencher.

Experiments described earlier showed that the shape of the binding isotherm could be conveniently manipulated by adjusting the ratio between quencher and dye. The ability to vary the Q:D ratio allows us to avoid the common problem of rapid saturation associated with many one-component saccharide sensors. The effects of adjusting the *m*-BBVBP^{4+} Q:D ratio on glucose sensing were determined using each of the dyes in the study. The dyes tetrasodium pyrophosphate (TSPP) and metacryloxypropyltrimethoxysilane (MPTS) were selected to represent the generality of adjusting the Q:D ratio on isotherm linearity and magnitude and are shown in Fig. 12.

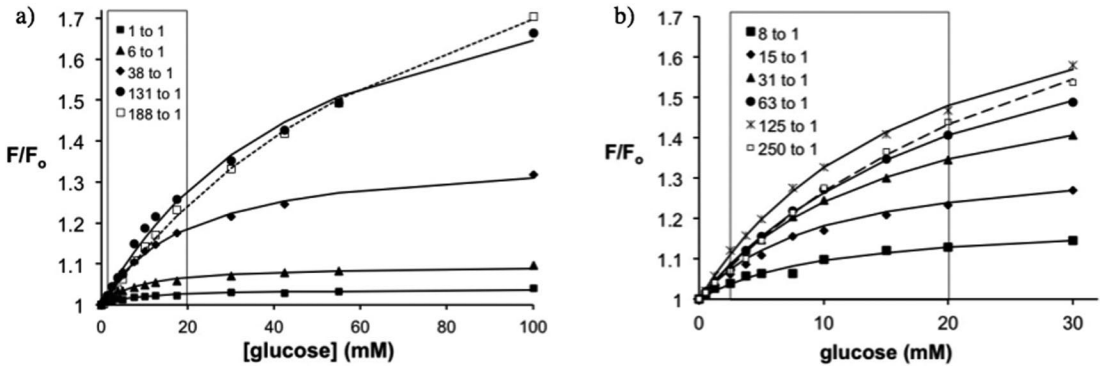

Fig. 12 Glucose response curves for addition of glucose to quenched solutions of dyes at pH 7.4 with varying *m*-BBVBP^{4+}:dye ratios. (a) TSPP; (b) MPTS. The dashed line with the hollow squares indicates the optimal Q:D ratio. The physiological glucose range is boxed. Dyes assessed at 4×10^{-6} M.

Q:D ratio optimization experiments were carried out for all of the dyes in the study to obtain the most dynamic, but linear signal responses possible in the physiological range. The optimized Q:D ratios and apparent glucose binding constants are given in Table 1 along with percentage increases in signals

observed after increasing the glucose concentration from 0 to 30 mM. For dyes that were only weakly quenched, such as sulforhodamine-B (SR-B), we generally had to use very high Q:D ratios to obtain linearity in the glucose response signal. Based on our quenching experiments, we expected to find a correlation between dye charge and glucose sensing ability. Generally, we observed that dyes with more anionic groups did provide stronger glucose signals and that the magnitude of signal response could be roughly correlated with the number of anionic groups on the dye (Fig. 13).

Table 1 Glucose-sensing data using anionic dyes with *m*-BBVBP^{4+}.

DYE	Optimal Q:D ratio	Apparent glucose binding constants at optimal Q:D ratio (K_{app}) (M^{-1})	% Signal increase from 0 to 30 mM
MPTS	250 to 1	38 ± 5	59
Fluorescein-SA	1300 to 1	22 ± 3	53
HPTS	31 to 1	27 ± 6	43
$HPTS(Lys)_3$	625 to 1	28 ± 5	42
TSPP	188 to 1	14 ± 4	33
PTCA	38 to1	50 ± 10	22
Lucifer yellow-I	1250 to 1	13 ± 3	16
APTS	13 to 1	30 ± 10	14
SR-B	125 000 to 1	23 ± 1	6

Optimal Q:D ratios for linear signal response to glucose in 0 to 30 mM concentration range and apparent glucose binding constants at that ratio.

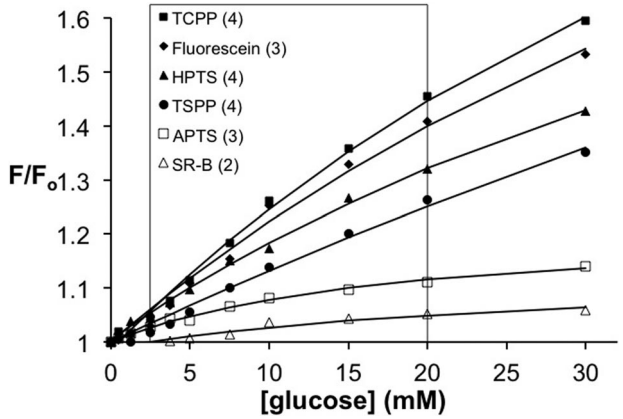

Fig. 13 Glucose response of selected dyes with *m*-BBVBP^{4+} at pH 7.4. F_o = initial quenched fluorescence, F = new fluorescence after addition. Dyes were [4×10^{-6} M] except SR-B which was [1×10^{-7} M]. The number of anionic groups is given in parentheses next to the dye name. The physiological glucose range is boxed. Note: 10 mM [glucose] = 180 mg/dL.

Overall, the demonstrated operational spectral range of our two-component system may be described as the entire visible portion of the spectrum. The generality of this two-component sensing system and the ease with which desired fluorophores can be introduced into the sensing scheme allows for considerable versatility in the design of saccharide-sensing systems. The flexibility demonstrated here suggested that multiple dyes could be used simultaneously in several interesting configurations.

Simultaneous use of multiple fluorescent dyes for glucose sensing

The simultaneous use of multiple dyes offers several potential advantages and applications for monosaccharide sensing. Significantly, in cases where more than one dye is used, several distinct emission wavelengths can be monitored for changes in response to glucose. Additionally, if one of the dyes used is nonresponsive to the analyte, and has its emission separated from those of other responsive dyes, then this multiple dye configuration can be used to provide so-called ratiometric sensing. In this case, the nonresponsive dye functions as a kind of check on changes in fluorescence that might be caused by factors other than changes in analyte concentration. These might include factors such as sample dilution, fluctuations in excitation lamp intensity, changes in the optical density, etc. A number of studies were conducted to demonstrate how simultaneous use of multiple dyes could help to realize some of these advantages [39].

Ratiometric fluorescent sensing

In our initial studies on the simultaneous use of multiple dyes, we utilized the porphyrin dye, TSPP, in combination with HPTS. Both of these dyes can be excited at 414 nm. In this two-dye study, we decided to use *m*-BBV^{2+} as the boronic acid receptor/quencher component. When the two-dye solution was treated with *m*-BBV^{2+}, the emission of both dyes was readily quenched to similar levels. When this quenched solution was titrated with glucose, both emission peaks showed a strong fluorescence increase. We decided that we could exploit this use of multiple dyes still further by including a nonresponsive reference dye into the configuration to provide a ratiometric sensing system.

As the method's name suggests, in ratiometric sensing, a ratio of emission intensities is used to provide a measure of whatever concentration or event is being monitored. When appropriate emissions are monitored, this method can improve the reliability of the sensing measurement. The most convenient choice as a reference dye was to select one that we had previously tested and determined to be insensitive to quenching (and thus glucose fluctuations) at the quencher concentration range used in these ratiometric experiments. We selected SR-B. Earlier Q:D ratio experiments had determined that an extraordinarily high Q:D ratio, ~100 000 to 1, was required to bring about even the slightest quenching of the SR-B fluorescence. Thus, so long as a Q:D ratio less than 100 000 to 1 was used, SR-B could function as a nonresponsive reference dye. SR-B has its peak excitation at 565 nm and, with only a small Stokes' shift, an emission at 580 nm in pH 7.4 buffer. Conveniently, SR-B does have a small degree of absorbance in the region of 410–420 nm, allowing for its use with similarly excitable dyes while using only a single excitation wavelength.

HPTS and TSPP were used as reporter dyes in combination with the SR-B as a reference dye. When the solution containing the three dyes was titrated with quencher solution, both the reporter dyes exhibited sensitivity to quenching by *m*-BBV^{2+} that was essentially the same as that observed in the absence of the reference dye. The reference dye itself showed only a small decrease in intensity, most likely owing to the slight effect of dilution on the dye emission (Fig. 14).

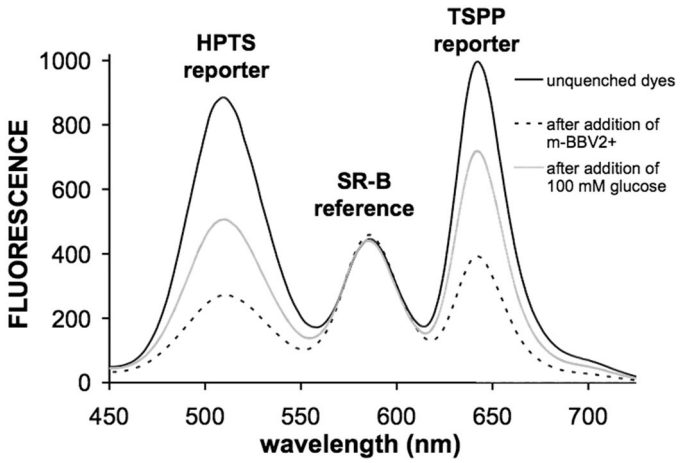

Fig. 14 Combined emission spectra of SR-B (1.3×10^{-7} M) (Q:D = 31 300:1); HPTS (6×10^{-8} M) (Q:D = 4170:1); and TSPP (4×10^{-6} M) (Q:D = 64:1) at pH 7.4 in response to addition of *m*-BBV^{2+} quencher and then 100 mM glucose. λ_{ex} = 414 nm.

The emission of both reporter dyes was then corrected in consideration of changes in the reference dye emission. The corrected emission intensity of the reporter dye is determined using eq. 1, where F is equal to the final fluorescence intensity and F_o is equal to the initial fluorescence intensity.

$$F/F_{o(\text{corrected})} = (F/F_{o(\text{reporter})})/(F/F_{o(\text{reference})}) \quad (1)$$

This provides a means for correcting the emission of both dyes for the aforementioned effects of dilution, lamp intensity fluctuation, etc. In a medical device, such corrections could be made with the aid of a simple processor. We corrected the raw signals for TSPP and HPTS using the reference signal from SR-B. The raw and corrected binding curves of both HPTS and TSPP reporter dyes are given in Fig. 15.

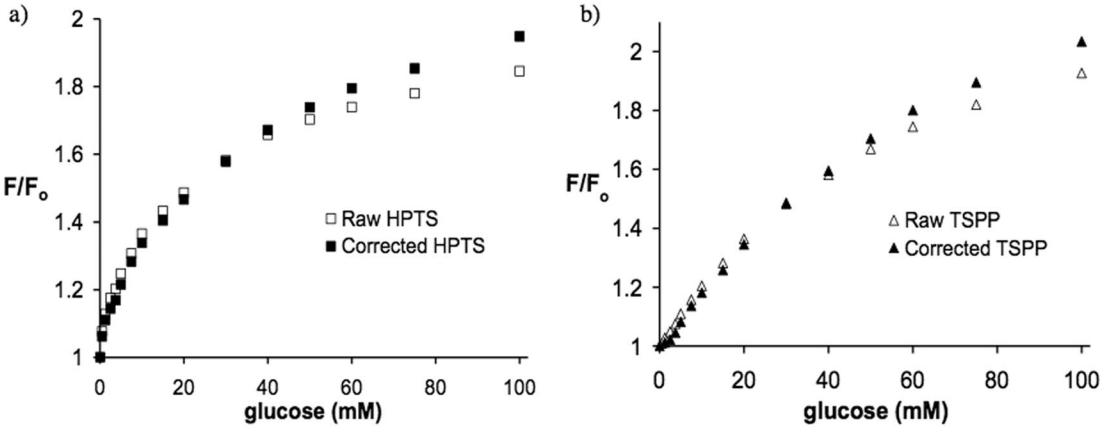

Fig. 15 Corrected and uncorrected binding curves of (a) HPTS (1.3×10^{-7} M) and (b) TSPP (3.9×10^{-6} M) at pH 7.4 in response to addition of *m*-BBV^{2+} quencher and then 100 mM glucose. λ_{ex} = 414 nm.

Using quantum dots as the fluorophore component

Over the past 20 years, the field of nanoscience has grown dramatically and advances in nanotechnology have been applied to electronics, optical devices, and sensors with extraordinary results. Fluorescent QDs are among the most remarkable and iconic of nanomaterials ever prepared. When compared with traditional fluorescent organic dyes, QDs possess advantages of photostability, optical tunability, and intense brightness [40,41]. QDs have found increasing use as replacements for traditional organic fluorophores in applications such as biomolecule tagging, tissue imaging, and ion sensing [42–47]. Surprisingly, however, by 2006 no methods for glucose detection utilizing inherently fluorescent QDs had been reported.

Fluorescent QDs are typically constructed of inorganic semiconductor core materials such as CdTe and CdSe, coated with an insulating shell material such as ZnS and further modified to provide desired surface chemistry. To prepare water-soluble core-shell QDs, surface functionalization with phosphonate, carboxyl, or amine groups is often employed. The particular surface chemistry allows for the QDs to bind to molecules of interest such as proteins and also determines their solubility, aggregation behavior, and sensitivity to quenching processes. Several groups have observed quenching of QD fluorescence using methyl viologen (MV^{2+}) [42,48–50]. The process is believed to occur through excited-state electron transfer from the QD to the viologen resulting in reduction of the viologen to $MV^{\bullet+}$.

We reasoned that water-soluble fluorescent QDs bearing such polar surface groups might be suitable replacements for traditional fluorescent organic dyes in our sensing system. The putative mechanism for glucose sensing with QDs and a boronic acid-substituted viologen quencher/receptor is shown in Scheme 3.

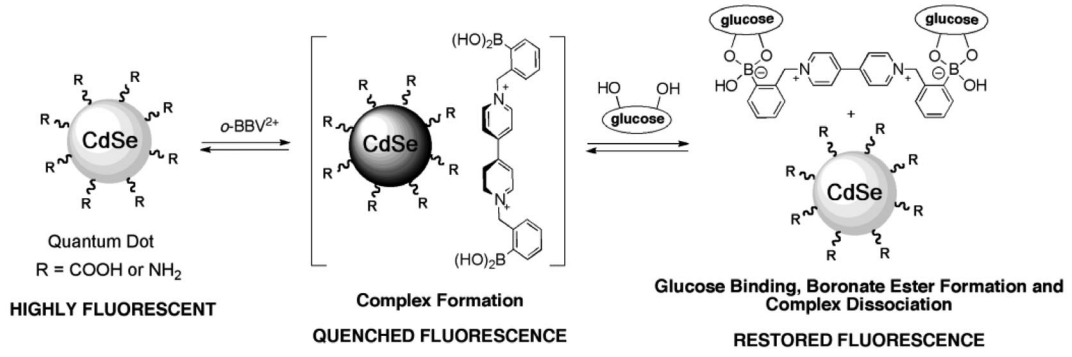

Scheme 3 Putative mechanism for glucose sensing with fluorescent QDs.

For our experiments, we used two sets of commercially available core-shell CdSe QDs coated with ZnS and identically prepared except for their surface functionalization. One set was prepared with carboxyl groups on the surface, and the other with amine groups. Both sets had broad absorption profiles and a fairly narrow fluorescence emission centered at 604 nm. We observed that these QDs functioned in our system in a manner similar to that of organic dyes: showing a decrease in fluorescence upon addition of *o*-BBV^{2+}, with the carboxyl-substituted QDs showing a stronger sensitivity to quenching than the amine-substituted QDs. Significantly, we also observed a robust fluorescence recovery on addition of glucose to the quenched QD solutions [51].

We then began a set of experiments to optimize the quencher-to-QD ratio and response of the quenched QDs to glucose. Previous studies had shown that choice of an appropriate quencher-to-fluorophore ratio was critical for a strong and linear signal response across the physiological glucose range. When experimenting with several different quencher-to-QD ratios, we observed generally the same

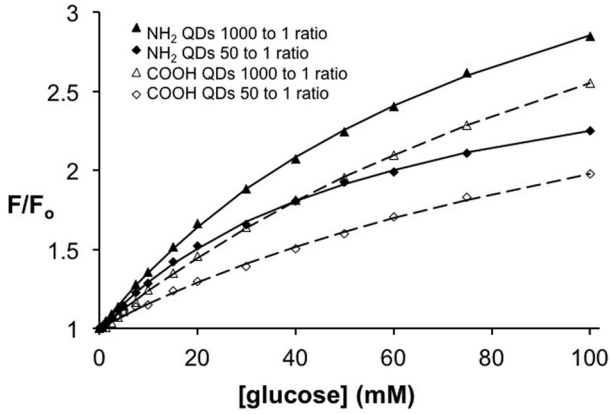

Fig. 16 Glucose response curves obtained using *o*-BBV^{2+} quenching the fluorescence of amine- and carboxyl-substituted QDs (5×10^{-8} M) at pH 7.4.

behavior as with traditional organic dyes where higher ratios tended to give larger, more linear fluorescence signals in response to addition of glucose (Fig. 16).

We screened both sets of QDs for glucose response at quencher-to-QD ratios of 50, 200, 500, and 1000 to 1. For both the amine- and carboxyl-substituted QDs, we obtained our best results using the 1000:1 quencher-to-QD ratio. Significantly, the use of QDs allows for a large signal response and a considerable degree of recovery of the initial, unquenched QD fluorescence after addition of 100 mM glucose. Since this initial report, a number of new QD-based glucose sensors have been reported, including a remarkable system capable of intracellular glucose sensing [52–59].

Immobilizing fluorophore and quencher in a hydrogel-sensing ensemble

For a glucose sensor to be useful in a device, the components must be immobilized for real-time sensing. Thus, our strategy was to incorporate the boronic acid quencher and dye components of our two-component system into a hydrogel polymer to prepare a sensor capable of detecting reversible changes in the glucose concentration. Based on our initial studies, an HPTS derivative was envisioned that contained both polymerizable groups and negative charges. This trisulfonamide compound, $HPTS(LysMA)_3$, could be prepared in moderate yield using lysine and methyl methacrylate as key reactants. In parallel work, a polymerizable derivative of the bipyridinium quencher *m*-$BBVBP^{4+}$ was also prepared. This quencher monomer, called BP^{4+}, with its two boronic acid receptors and a charge of 4+, was expected to deliver significant quenching. Both polymerizable components were evaluated in solu-

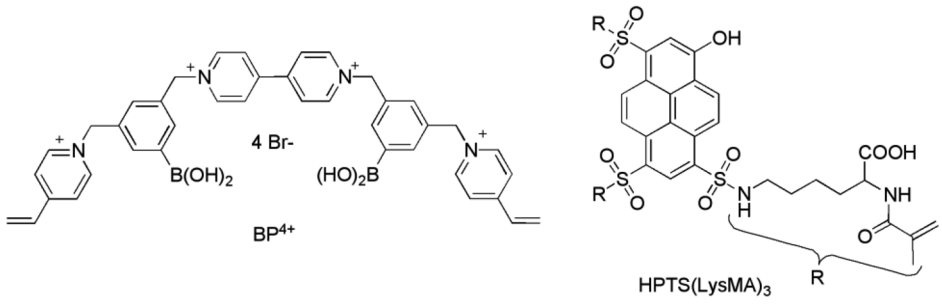

Fig. 17 Polymerizable dye and quencher components: $HPTS(LysMA)_3$ and BP^{4+}.

tion studies for quenching and sugar-sensing ability. The dye and quencher monomers are shown in Fig. 17.

Immobilization of sensing components

To prepare an appropriately hydrophilic and permeable sensing hydrogel, we relied on the simple method of copolymerization of our dye and quencher monomers with 2-hydroxyethyl methacrylate (HEMA), polyethyleneglycol dimethacrylate (PEG-DMA), and the initiator VA-044. In a typical polymerization, we would prepare a 50 % aqueous solution containing HEMA, PEGDMA, VA-044, and the quencher and dye monomers. This mixture was then cooled on ice and deaerated. Operating in an argon atmosphere, the deaerated mixture was then injected between two glass plates separated by a Teflon spacer and held together in a steel mold. The thickness of the Teflon spacer controls the thickness of the resultant hydrogel. After injection of the monomer mixture into the mold, the apparatus was then sealed in a plastic bag and placed in an oven. Free-radical polymerization of the mixture was carried out at 40 °C for ~15 h to produce the desired sensing hydrogel. This process is represented in Scheme 4.

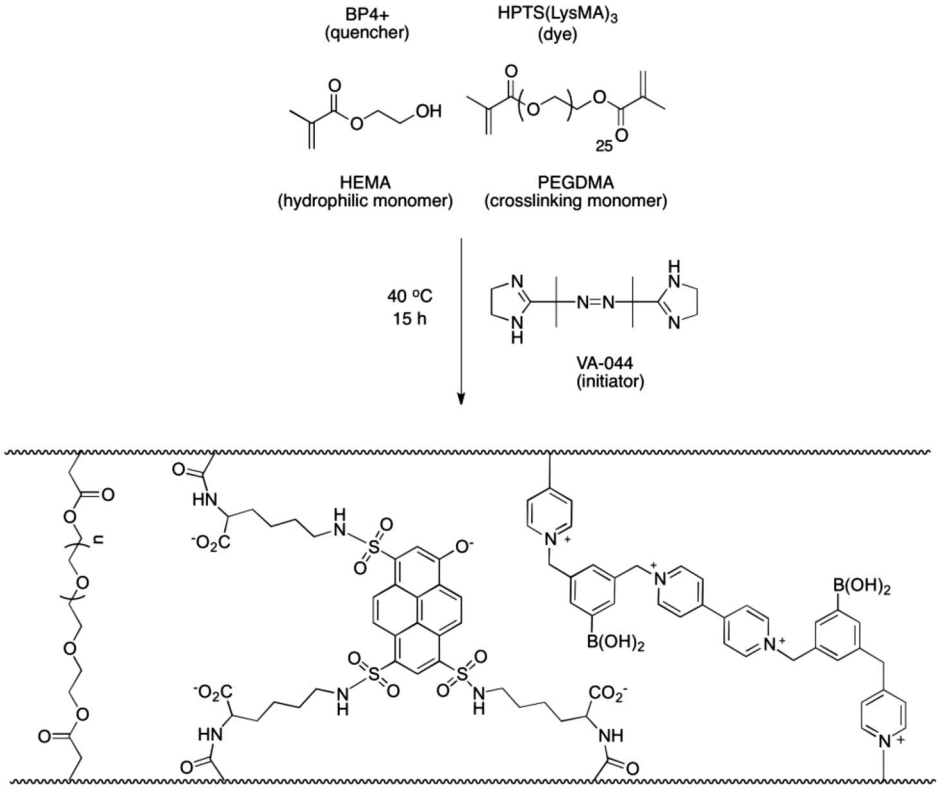

Scheme 4 Preparation of a glucose-sensing hydrogel through free-radical polymerization.

The slightly orange-colored hydrogel films prepared using this method were typically allowed to equilibrate in pH 7.4 buffer and then assessed for their response to changes in glucose concentration. To evaluate this response, a hydrogel would be mounted into a flow cell and phosphate buffer of ionic strength 0.1 M circulated through the cell. To mimic physiological conditions more closely, we maintained the temperature of the circulating solution at the physiological body temperature of 37 °C. By

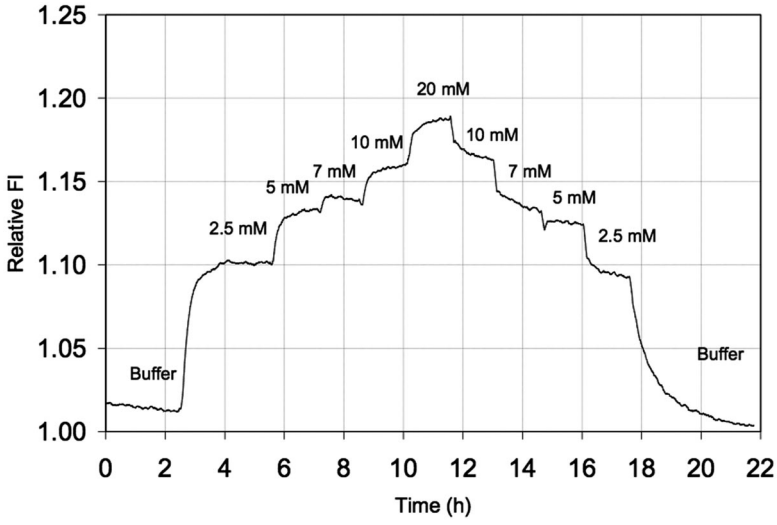

Fig. 18 Continuous glucose-sensing profile of a 0.001" hydrogel containing BP^{4+} and $HPTS(LysMA)_3$ at pH 7.4 and 37 °C. λ_{ex} = 470 nm and λ_{em} = 540 nm.

raising and then lowering the concentration of the circulating glucose solution we could detect real-time increases and decreases in glucose concentration. An example of such reversible, real-time sensing was obtained using a .001-inch-thick hydrogel and is shown as a 22-h sensing profile in Fig. 18 [60].

Significantly, these hydrogels showed fairly rapid responses to changes in the glucose concentration and showed a good return to baseline after the glucose concentration was returned to 0 mM. Similar profiles were obtained when measuring changes in concentration of fructose and galactose. Since these initial experiments on immobilizing the system for reversible real-time glucose sensing, considerable work has been done to improve performance of the hydrogels through modifications and substitutions of the quencher and dye monomers. For example, considerable improvement in hydrogel performance was achieved through use of a polymerizable version of aminopyrenetrisulfonic acid (APTS) in which the dye was more loosely tethered to the sensing polymer through a single covalent attachment [61,62]. The immobilized sensing system was also deployed in an easy-to-use and fairly portable sensing configuration in which a small piece of hydrogel was attached to the end of a fiber-optic cable [61,63]. Most recently, a remarkable application of the immobilized system was reported in which the sensing elements were immobilized in hydrogel form in multiwell plates for high-throughput screening applications [64].

CONCLUSION

The object of this review was to trace major developments, largely in our own research program, which led from the initial observation of the exceptional sugar signaling of *o*-BBV-HPTS system to the present time when we have several two-component sensing configurations and probes for the detection of sugars in biological fluids. In this review, particular emphasis has been given to the development of the two-component boronic acid-based fluorescent sugar sensors. As the preceding examples illustrate, this two-component glucose-sensing system is extraordinarily flexible in terms of the many ways in which it can be configured. Indeed, new system applications and improved sensing capabilities based on the fundamental two-component approach appear in the literature on a regular basis. Most importantly, though, these sensing capabilities have contributed significantly to both the basic science of fluores-

cence-based sensor chemistry and to improving methods for detection of glucose and other carbohydrates.

ACKNOWLEDGMENTS

We thank GluMetrics, Inc., operating through the UC BioStar Industry–University Cooperative Research program (Grant bio04-10458), for financial support.

REFERENCES

1. K. E. Toghill, R. G. Compton. *Int. J. Electrochem. Sci.* **5**, 1246 (2010).
2. M. S. Steiner, A. Duerkop, O. S. Wolfbeis. *Chem. Soc. Rev.* **40**, 4805 (2011).
3. J. P. Lorand, J. O. Edwards. *J. Org. Chem.* **24**, 769 (1959).
4. D. G. Hall. In *Boronic Acids, Preparation and Applications in Organic Synthesis and Medicine*, D. G. Hall (Ed.), pp. 1–99, Wiley-VCH, Weinheim (2005).
5. G. Springsteen, B. H. Wang. *Tetrahedron* **58**, 5291 (2002).
6. T. D. James, K. Sandanayake, S. Shinkai. *Angew. Chem., Int. Ed. Engl.* **35**, 1910 (1996).
7. S. L. Wiskur, J. J. Lavigne, H. Ait-Haddou, V. Lynch, Y. H. Chiu, J. W. Canary, E. V. Anslyn. *Org. Lett.* **3**, 1311 (2001).
8. W. J. Ni, H. Fang, G. Springsteen, B. H. Wang. *J. Org. Chem.* **69**, 1999 (2004).
9. J. Yan, G. Springsteen, S. Deeter, B. H. Wang. *Tetrahedron* **60**, 11205 (2004).
10. Z. Sharrett, S. Gamsey, J. Fat, D. Cunningham-Bryant, R. A. Wessling, B. Singaram. *Tetrahedron Lett.* **48**, 5125 (2007).
11. H. Fang, G. Kaur, B. H. Wang. *J. Fluoresc.* **14**, 481 (2004).
12. J. Yoon, A. W. Czarnik. *J. Am. Chem. Soc.* **114**, 5874 (1992).
13. T. D. James, P. Linnane, S. Shinkai. *Chem. Commun.* 281 (1996).
14. O. Rusin, O. Alpturk, M. He, J. O. Escobedo, S. Jiang, F. Dawan, K. Lian, M. E. McCarroll, I. M. Warner, R. M. Strongin. *J. Fluoresc.* **14**, 611 (2004).
15. H. Eggert, J. Frederiksen, C. Morin, J. C. Norrild. *J. Org. Chem.* **64**, 3846 (1999).
16. J. D. Larkin, K. A. Frimat, T. M. Fyles, S. E. Flower, T. D. James. *New J. Chem.* **34**, 2922 (2010).
17. J. F. Wang, S. Jin, S. Akay, B. H. Wang. *Eur. J. Org. Chem.* 2091 (2007).
18. R. Badugu, J. R. Lakowicz, C. D. Geddes. *J. Fluoresc.* **14**, 617 (2004).
19. H. S. Cao, D. I. Diaz, N. DiCesare, J. R. Lakowicz, M. D. Heagy. *Org. Lett.* **4**, 1503 (2002).
20. S. Arimori, H. Murakami, M. Takeuchi, S. Shinkai. *J. Chem. Soc., Chem. Commun.* 961 (1995).
21. G. Springsteen, B. H. Wang. *Chem. Commun.* 1608 (2001).
22. J. N. Camara, J. T. Suri, F. E. Cappuccio, R. A. Wessling, B. Singaram. *Tetrahedron Lett.* **43**, 1139 (2002).
23. E. B. de Borba, C. L. C. Amaral, M. J. Politi, R. Villalobos, M. S. Baptista. *Langmuir* **16**, 5900 (2000).
24. K. Nakashima, N. Kido. *Photochem. Photobiol.* **64**, 296 (1996).
25. Z. G. Zhao, T. Shen, H. J. Xu. *J. Photochem. Photobiol., A* **52**, 47 (1990).
26. B. S. Gaylord, S. J. Wang, A. J. Heeger, G. C. Bazan. *J. Am. Chem. Soc.* **123**, 6417 (2001).
27. D. L. Wang, X. Gong, P. S. Heeger, F. Rininsland, G. C. Bazan, A. J. Heeger. *Proc. Natl. Acad. Sci. USA* **99**, 49 (2002).
28. L. H. Chen, D. W. McBranch, H. L. Wang, R. Helgeson, F. Wudl, D. G. Whitten. *Proc. Natl. Acad. Sci. USA* **96**, 12287 (1999).
29. N. DiCesare, M. R. Pinto, K. S. Schanze, J. R. Lakowicz. *Langmuir* **18**, 7785 (2002).
30. J. T. Suri, D. B. Cordes, F. E. Cappuccio, R. A. Wessling, B. Singaram. *Langmuir* **19**, 5145 (2003).

31. S. Gamsey, N. A. Baxter, Z. Sharrett, D. B. Cordes, M. M. Olmstead, R. A. Wessling, B. Singaram. *Tetrahedron* **62**, 6321 (2006).
32. S. Gamsey, A. Miller, M. M. Olmstead, C. M. Beavers, L. C. Hirayama, S. Pradhan, R. A. Wessling, B. Singaram. *J. Am. Chem. Soc.* **129**, 1278 (2007).
33. Z. Sharrett, S. Gamsey, P. Levine, D. Cunningham-Bryant, B. Vilozny, A. Schiller, R. A. Wessling, B. Singaram. *Tetrahedron Lett.* **49**, 300 (2008).
34. A. Schiller, R. A. Wessling, B. Singaram. *Angew. Chem., Int. Ed.* **46**, 6457 (2007).
35. A. Schiller, B. Vilozny, R. A. Wessling, B. Singaram. *Anal. Chim. Acta* **627**, 203 (2008).
36. B. Vilozny, A. Schiller, R. A. Wessling, B. Singaram. *Anal. Chim. Acta* **649**, 246 (2009).
37. D. B. Cordes, S. Gamsey, Z. Sharrett, A. Miller, P. Thoniyot, R. A. Wessling, B. Singaram. *Langmuir* **21**, 6540 (2005).
38. D. B. Cordes, A. Miller, S. Gamsey, Z. Sharrett, P. Thoniyot, R. Wessling, B. Singaram. *Org. Biomol. Chem.* **3**, 1708 (2005).
39. D. B. Cordes, A. Miller, S. Gamsey, B. Singaram. *Anal. Bioanal. Chem.* **387**, 2767 (2007).
40. A. Rogach (Ed.). *Semiconductor Nanocrystal Quantum Dots: Synthesis, Assembly, Spectroscopy and Applications*, Springer-Verlag, New York (2008).
41. M. Bruchez Jr., M. Moronne, P. Gin, S. Weiss, A. P. Alivisatos. *Science* **281**, 2013 (1998).
42. D. Ishii, K. Kinbara, Y. Ishida, N. Ishii, M. Okochi, M. Yohda, T. Aida. *Nature* **423**, 628 (2003).
43. D. R. Larson, W. R. Zipfel, R. M. Williams, S. W. Clark, M. P. Bruchez, F. W. Wise, W. W. Webb. *Science* **300**, 1434 (2003).
44. W. C. W. Chan, D. J. Maxwell, X. H. Gao, R. E. Bailey, M. Y. Han, S. M. Nie. *Curr. Opin. Biotechnol.* **13**, 40 (2002).
45. W. C. W. Chan, S. M. Nie. *Science* **281**, 2016 (1998).
46. C. M. Niemeyer. *Angew. Chem., Int. Ed.* **40**, 4128 (2001).
47. M. Green. *Angew. Chem., Int. Ed.* **43**, 4129 (2004).
48. S. Logunov, T. Green, S. Marguet, M. A. El-Sayed. *J. Phys. Chem. A* **102**, 5652 (1998).
49. Y. Nosaka, H. Miyama, M. Terauchi, T. Kobayashi. *J. Phys. Chem.* **92**, 255 (1988).
50. D. Duonghong, E. Borgarello, M. Gratzel. *J. Am. Chem. Soc.* **103**, 4685 (1981).
51. D. B. Cordes, S. Gamsey, B. Singaram. *Angew. Chem., Int. Ed.* **45**, 3829 (2006).
52. J. Tanne, D. Schafer, W. Khalid, W. J. Parak, F. Lisdat. *Anal. Chem.* **83**, 7778 (2011).
53. P. Wu, Y. He, H. F. Wang, X. P. Yan. *Anal. Chem.* **82**, 1427 (2010).
54. R. Freeman, L. Bahshi, T. Finder, R. Gill, I. Willner. *Chem. Commun.* 764 (2009).
55. W. T. Wu, T. Zhou, J. Shen, S. Q. Zhou. *Chem. Commun.* 4390 (2009).
56. A. D. Saran, M. M. Sadawana, R. Srivastava, J. R. Bellare. *Colloids Surf., A* **384**, 393 (2011).
57. M. Zheng, Y. Cui, X. Y. Li, S. Q. Liu, Z. Y. Tang. *J. Electroanal. Chem.* **656**, 167 (2011).
58. X. Y. Li, Y. L. Zhou, Z. Z. Zheng, X. L. Yue, Z. F. Dai, S. Q. Liu, Z. Y. Tang. *Langmuir* **25**, 6580 (2009).
59. H. S. Mader, O. S. Wolfbeis. *Microchim. Acta* **162**, 1 (2008).
60. J. T. Suri, D. B. Cordes, F. E. Cappuccio, R. A. Wessling, B. Singaram. *Angew. Chem., Int. Ed.* **42**, 5857 (2003).
61. S. Gamsey, J. T. Suri, R. A. Wessling, B. Singaram. *Langmuir* **22**, 9067 (2006).
62. Z. Sharrett, S. Gamsey, L. Hirayama, B. Vilozny, J. T. Suri, R. A. Wessling, B. Singaram. *Org. Biomol. Chem.* **7**, 1461 (2009).
63. P. Thoniyot, F. E. Cappuccio, S. Gamsey, D. B. Cordes, R. A. Wessling, B. Singaram. *Diabetes Technol. Therapeutics* **8**, 279 (2006).
64. B. Vilozny, A. Schiller, R. A. Wessling, B. Singaram. *J. Mater. Chem.* **21**, 7589 (2011).

